Desalination and Water Treatment
www.deswater.com
doi: 10.1080/19443994.2013.793947

51 (2013) 7764–7774
December

Taylor & Francis
Taylor & Francis Group

Adsorption and desorption studies on the performance of Fe–loaded chitosan carbonized rice husk for metal ion removal

Sivaraju Sugashini, Khadhar Mohamed Meera Sheriffa Begum*

Department of Chemical Engineering, National Institute of Technology, Tiruchirappalli 15, Tamil Nadu, India
Tel. +91 431 2503109; Fax: +91 431 2500133; email: meerasheriffa@gmail.com

Received 2 May 2012; Accepted 6 March 2013

ABSTRACT

Reuse of agro-waste into useful adsorbents like activated carbon has considerable attention in waste water treatment. Usually the activation of carbon is done by treating it with inorganic chemicals, polymers, biopolymers, etc. This paper deals with the preparation of novel Fe–loaded chitosan carbonized rice husk beads (Fe–CCRB) by blending Fe (metal)–loaded chitosan (organic compound) and carbonized rice husk. The prepared Fe–CCRB was used for the removal of metal ion. The surface properties of the adsorbent were characterized by scanning electron microscopy (SEM), Fourier transform infrared spectroscopy (FTIR) and Brauner–Emmett–and Teller (BET) analyzer. The effects of process variables, such as contact time, agitation speed, initial metal ion concentration, adsorbent dosage, pH, and temperature of the solution using Fe–CCRB were studied. Various isotherms and kinetic models were fitted with experimental data to describe the behavior of diffusion mechanism, solute interaction, and nature of adsorption with the adsorbent through batch studies. Mass transfer and thermodynamic characteristics were also evaluated. Regeneration studies were attempted to check the stability and activity of the adsorbent.

Keywords: Rice husk carbon; Iron–loaded chitosan; Adsorption; Mass transfer diffusion; Regeneration

1. Introduction

The presence of heavy metals in the waste water produced by various industries is accumulating in the ecosystem which causes serious risk to the environment and endangers public health. Among various toxic heavy metals, chromium is the most important because of its carcinogenic nature and also wide application in industries. Chromium exists in two forms viz Cr (III) ions and Cr (VI) ions, which are generated from various industrial processes, such as electroplating, leather tanning, mining, dyes and pigments, steel fabrication, canning industries, etc. [1,2]. Cr (III) ions are nontoxic and play an essential role in the metabolism of plant and animals. Cr (VI) ions are highly toxic. Inhalation of Cr (VI) ions leads to the carcinogenic problem. Other health effects of Cr (VI) ions are the skin allergy and liver problems.

Due to its severe toxicity, Environmental Protection Agency Cincinaati OH USA, set the tolerance limit for the discharge of Cr (VI) ions into surface water to 0.1 mg/l and in potable water to 0.05 mg/l [3]. Thus, the removal of Cr (VI) ions becomes mandatory. Various methodologies have been used for the

*Corresponding author.

removal of Cr (VI) ions like electrochemical, ion exchange, membrane filtration, reverse osmosis, and chemical coagulation, etc. [4]. However, each method has its shortcomings and limitations.

One of the most efficient and commercialized method is adsorption due to its simplicity, sludge free operation, easiness in handling, availability of various adsorbents, and more efficient in removal of heavy metals at lower concentration levels [5].

Several investigators reported different adsorbents for the removal of Cr (VI) ions, such as activated carbon [4–6], chiotsan [7], biosorbents [8], polymeric compounds [9], etc. Activated carbon is a common adsorbent because of its high surface area and easy availability. However, commercial activated carbon is highly expensive. This in turn led to finding an alternate way for preparing the activated carbon at low cost using waste biomass. Rice husk is one of the cheapest and abundantly available biomass in which the constituents of rice husk are silica (20%), cellulose (40%), hemicellulose (20%), and lignin (20%) used for the preparation of carbon [10–15].

In recent years, surface-modified activated carbon was prepared to improve the adsorption capacity and removal efficiency of metals ions [16–18]. Chitosan, a biopolymer of glucosamine has received considerable attention for the removal of transition metal ions and organic species due to its excellent metal chelating property and availability [19–21]. In addition to that, metallo–organic chelating compounds are used in waste water treatment. One of these types of metallo–organic chelating materials is transition metals–chitosan complexes. Recent investigations show that the amine and hydroxyl groups in the chitosan chelates Fe (III) ions and more than one polymer chain is involved in the formation of complexes [22–24]. Metallo–organic chelating materials are more effective when cross-linked after metal complexation. Cross-linking agents like glutaraldehyde, epichlorohydrin, etc. are used to enhance the stability of chitosan in acidic medium by forming Schiff-base reactions [25–27]. It is desirable to have the knowledge of using carbon metallo–organic composites in order to minimize the excess organic reagents used for the purification of adsorbents.

Thus, this present study intends to investigate the preparation of metallo–organic carbon beads by using rice husk as a precursor for carbon and iron–loaded chitosan as metallo–organic complex. The synthesized Fe–loaded chitosan carbonized rice beads (Fe–CCRB) was applied for the removal of hexavalent chromium.

2. Materials and methods

2.1. Reagents

Raw rice husk was obtained from a local rice mill. Chitosan was purchased from Pelican Biotech industry, India. The chemicals used in this study, such as nitric acid, sulphuric acid, acetic acid, sodium hydroxide, acetone, $FeCl_3$, etc., were supplied by Merck, India. Potassium dichromate was used for the preparation of Cr (VI) stock solution. The AR grade of 1,5-diphenyl carbazide was used for analyzing chromium. Glutaraldehyde was used as cross-linking agent supplied by Merck, India. Double distilled water was used to prepare all the solutions.

2.2. Preparation of carbonized rice husk (CRH)

The procedure for the preparation of rice husk has been reported in our earlier literature [27]. According to the procedure, rice husk was thoroughly washed with distilled water and dried in hot air oven at 100°C for 5 h. The dried sample was treated with 70% concentrated nitric acid (1:1 by weight) at 70°C for 1½ h in order to reduce the silica content [28]. After acid treatment, the sample was kept for overnight and then subjected to heat under a controlled atmosphere of nitrogen from ambient temperature to 600°C at a constant heating rate of 5°C min^{-1} in a tubular furnace for 4 h. The prepared carbonized rice husk (CRH) was cooled in desiccator and stored.

2.3. Preparation of Fe–loaded chitosan (Fe–C) gel

Fe–loaded chitosan (Fe–C) gel was prepared by dissolving 1 g of chitosan in 50 ml of 0.1 M $FeCl_3$ and kept in rotary shaker for 2 h.

2.4. Preparation of Fe–loaded chitosan carbonized rice husk beads (Fe–CCRB)

One gram of CRH was added to the Fe–C gel and kept in a rotary shaker for 3 h at 200 rpm. The Fe–loaded chitosan carbon gel solution was dropped into 0.5 mol/L of NaOH solution which remained for 12 h and washed with distilled water to remove excess NaOH. Then 7.5% glutaraldehyde in ethanol was added to the beads which remained for 24 h, then washed, and dried.

2.5. Characterization of Fe–CCRB

The specific surface area of Fe–CCRB was measured using BET analyzer. The morphological structure was observed by Scanning electron micro-

scope (Hitachi S3000H). FTIR spectra were recorded using FTIR spectrophotometer (Perkin Elmer, spectrum RXI) to analyze the presence of activation in the adsorbent.

2.6. Adsorption studies

Batch adsorption studies were conducted to determine the adsorption capacity and percentage removal of Cr (VI) ions using Fe–CCRB. A desired quantity of Fe–CCRB was added to 25 ml of known concentration of Cr (VI) ions and pH in a 100 ml volumetric flask and kept in a rotary shaker at agitation speed of 200 rpm. The supernatant liquid samples were filtered periodically and then analyzed by using Jasco UV spectrophotometer at 540 nm to calculate the adsorption capacity and percentage removal efficiency. Experiments were repeated in triplicates and the average percentage deviation was found to be 3–5%. The amount of adsorption, q_t (mg/g) and percentage removal (%) were calculated using Eqs. (1) and (2).

$$q_t = \{(C_0 - C_t)V\}/m \quad (1)$$

$$\text{Percentage removal} = [(C_0 - C_F)/C_0] \times 100 \quad (2)$$

where C_0 and C_t are the initial concentration and concentration at any instant (mg/l), V is the volume of solution (l), q_t is the adsorption capacity (mg/g) at time t, m is the weight of adsorbent (g), and C_F is the solution concentration at the end of the adsorption process (mg/l).

2.7. Regeneration studies

Regeneration studies were conducted to test the reproducibility of the adsorbent. 0.5 g of spent adsorbent was agitated with 25 ml of NaOH solutions for 3 h. After desorption, the sample was washed and neutralized with distilled water. The regenerated adsorbent sample was reused in the next cycle of the adsorption experiments. The adsorption–desorption studies were conducted for three cycles.

3. Results and discussion

3.1. Characterization of adsorbents

The prepared Fe–CCRB adsorbents were characterized by BET, SEM, and FTIR analysis.

3.1.1. BET analysis

In general, any material deposited on the porous materials, such as activated carbon (carbonized biomass), the specific surface area is decreased [29]. The specific surface area of CRH (activated carbon) and Fe–CCRB were found to be 20 and 16 m^2/g, respectively. The results clearly indicated that the activation of Fe–C on carbonized rice husk did not affect the specific surface area significantly, which reveals that the porous nature of CRH is not affected while loaded with Fe–C.

3.1.2. SEM analysis

The surface morphology of Fe–CCRB was investigated using SEM and the SEM image of the Fe–CCRB particle is shown in Fig. 1, which gives the surface texture and porosity of the Fe–CCRB particle. The image reveals that the particles have a very narrow size distribution, spherical-shaped with very small cavities and rough surfaces. This may be due to the loading of biopolymer on insoluble materials (carbonized rice husk and Fe), which involves the suspension of biopolymer in aqueous solution and subsequent cross-linking.

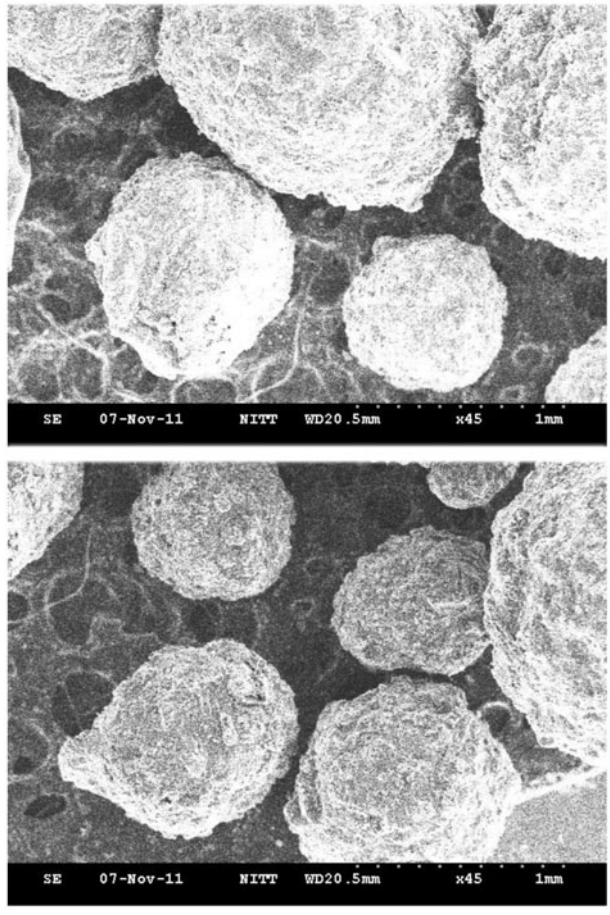

Fig. 1. SEM image of Fe–CCRB.

3.1.3. FTIR analysis

Fig. 2 shows the FTIR spectra of CRH, Fe–CCRB, and spent adsorbents. The presence of functional groups in the adsorbents is given in Table 1.

Initially the CRH shows peaks which are attributed to the presence of N–H groups. The formation of new peaks associated with the presence of carbonyls, carboxylic acid, and ketone groups were observed on deposition of Fe–C into CRH.

The functional groups like N–H stretching at 3399.34 cm^{-1} shifted to 3,209 cm^{-1}, C=O stretching mode in carbonyls, carboxylic acid, and ketones at 1617.60 cm^{-1} shifted to 1,605 cm^{-1}, C–N stretching at 1084.36 cm^{-1} shifted to 1803 cm^{-1}, NH_2 and NH wagging at 796 cm^{-1} shifted to 784.46 cm^{-1}, and the functional groups, such as C–O and O–H bending at 1,375.09 cm^{-1}, C–H groups at 681.05 cm^{-1} and 476.50 cm^{-1} were disappeared in the adsorbent after adsorption. The nature of shifting in peaks revealed that the Cr(VI) ions were attached to these groups.

3.2. Effect of contact time

The effect of contact time on adsorption capacity of Cr (VI) ions using Fe–CCRB was studied for 25 ml of 100, 300, and 500 ppm of initial metal ion concentration at 0.1 g of adsorbent dosage at 2.0 pH and agitation speed of 200 rpm in order to determine the equilibrium time. The results are shown in Fig. 3. It is observed that the rate of adsorption initially increased and then gradually remained constant with increase in contact time and reached equilibrium nearly at 150 min.

This may be due to the availability of a large number of vacant sites initially for adsorption, later the adsorption capacity tailed off due to the saturation of vacant sites.

3.3. Effect of agitation speed

The effect of agitation speed on adsorption capacity of Cr (VI) ions was studied by varying the agitation speed from 100 to 300 rpm for 25 ml of initial

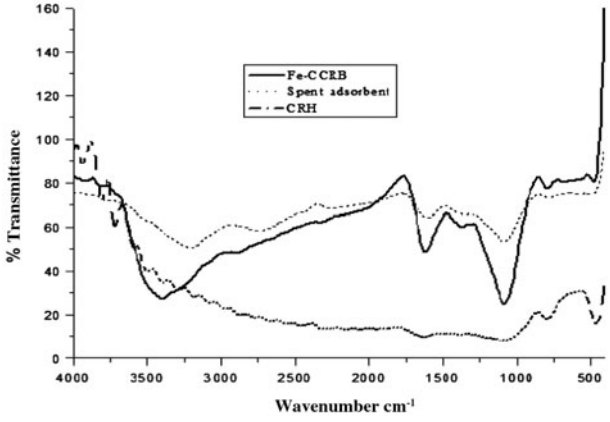

Fig. 2. FTIR spectra of CRH, Fe–CCRB and spent adsorbent.

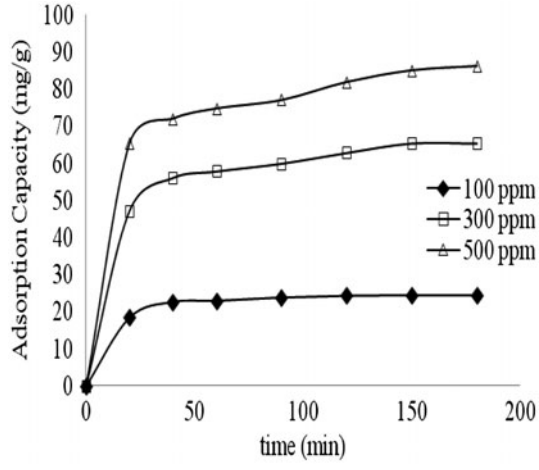

Fig. 3. Effect of contact time on adsorption capacity of Cr (VI) ions by Fe–CCRB (m = 0.1 g, v = 25 ml, speed = 200 rpm, pH 2).

Table 1
The functional groups present in CRH, Fe–CCRB, and spent adsorbent

Functional groups	CRH	Fe–CCRB	Spent adsorbent
O–H (H bonded) stretching	3,934.8 cm^{-1}	3,916.30 cm^{-1}	–
Hydroxyl and N–H stretching	3,396.04 cm^{-1} 3,291.76 cm^{-1}	3,399 cm^{-1}	3,209 cm^{-1}
N–H bending	2,062.3 cm^{-1}	–	–
C = O (stretching mode in carbonyls, carboxylic acid, and ketones)	–	1,617 cm^{-1}	1,605 cm^{-1}
C–O and O–H bending	–	1,375.09 cm^{-1}	–
C–N and C–O stretching	1,089.99 cm^{-1}	1,084.08 cm^{-1}	1,083 cm^{-1}
NH_2 and NH wagging	798.27 cm^{-1}	796 cm^{-1}	784.46 cm^{-1}
C–H groups out of plane deformation	462.10 cm^{-1}	681.05 cm^{-1} 476.10 cm^{-1}	–

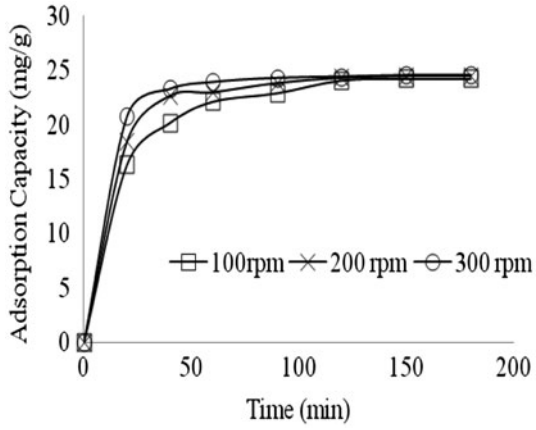

Fig. 4. Effect of agitation speed on adsorption capacity of Cr (VI) ions by Fe–CCRB ($m = 0.1$ g, $v = 25$ ml, $C_0 = 100$ mg/l, pH 2).

concentration of 100 ppm at pH 2 and adsorbent dosage of 0.1 g. The results are presented in Fig. 4. Initially the rate of adsorption was increased with increased agitation speed. The maximum adsorption capacity was obtained at 200 rpm beyond which the increase was not observed significantly. This is due to the contact between the metal ion and active sites developed when increasing the agitation speed. Hence, the equilibrium agitation speed was fixed at 200 rpm.

3.4. Effect of pH

The effect of pH on adsorption capacity of Cr (VI) ion using Fe–CCRB is shown in Fig. 5. The maximum percentage removal and adsorption capacity of Cr (VI) ion were obtained at pH 2. At pH 2, the Cr (VI) ions exist as hydrogen chromate ($HCrO_4^-$: 90%), dichromate ($Cr_2O_7^-$: 5%), and chromic acid (H_2CrO_4: 5%). At higher pH, the predominant species of Cr (VI) ion is CrO_4^{2-}. The surface positive functional groups of the Fe–CCRB adsorbent carried the oxyanions (negatively-charged) of Cr (VI) ions by electrostatic force of attraction [30,31].

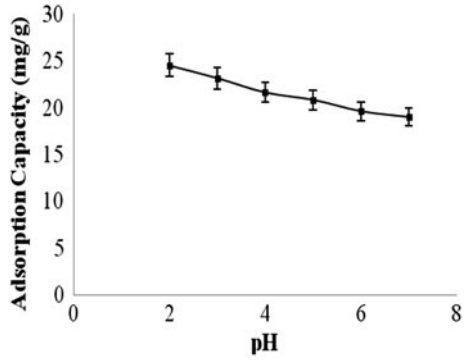

Fig. 5. Effect of pH on adsorption capacity of Cr (VI) ions by Fe–CCRB ($m = 0.1$ g, $v = 25$ ml, $C_0 = 100$ mg/l).

On the other hand, the physico-chemical properties of chitosan are depending on the chain length, charge density, and distribution regarding its cationic nature obtained during the degree of deacetylation. At neutral pH, about 50% of total amine groups remain protonated and theoretically available for the adsorption [32]. As the pH decreases, the protonation of the amino groups increased which increased the adsorption efficiency. The adsorption mechanism of Cr (VI) ions is considered as a ligand-exchange reaction between the coordinated nitrate and $HCrO_4^-$, and this reaction mechanism is represented in Scheme 1.

3.5. Effect of initial metal ion concentration

Fig. 6 represents the effect of initial metal ion concentration on adsorption capacity and percentage removal of Cr (VI) ion using Fe–CCRB. The adsorption capacity of Cr (VI) ions was increased and the percentage removal of Cr (VI) ions was decreased with increased metal ion concentrations.

The increase in adsorption capacity may be due to the higher adsorption rate and utilization of all active sites available for the adsorption at higher concentration and also, the higher initial adsorbate concentration provided higher driving force to overcome all mass transfer resistances of metal ions from the aqueous to solid phase resulting in higher probability of collision between Cr (VI) ions and the active sites. The decrease in percentage removal may be due to the limited number of actives sites in the adsorbent attaining saturation above certain concentration [33,34]. A maximum percentage removal of 98% at 100 ppm and adsorption capacity of 88 mg/g at 500 ppm were obtained.

3.6. Effect of temperature

The effect of temperature on adsorption of Cr (VI) ions was investigated by varying the temperature from 30 to 70°C as shown in Fig. 7.

The increase in adsorption capacity may be due to the formation of some new adsorption sites on the surface of the adsorbent with enlarged pores, and the increased rate of intraparticle diffusion of Cr (VI) ions into the pores of Fe–CCRB at higher temperature leads to the endothermic adsorption [35].

3.7. Adsorption isotherms and chi square analysis

Various isotherms like Freundlich, Langmuir, Temkin, and Redlich Peterson isotherms [36] were

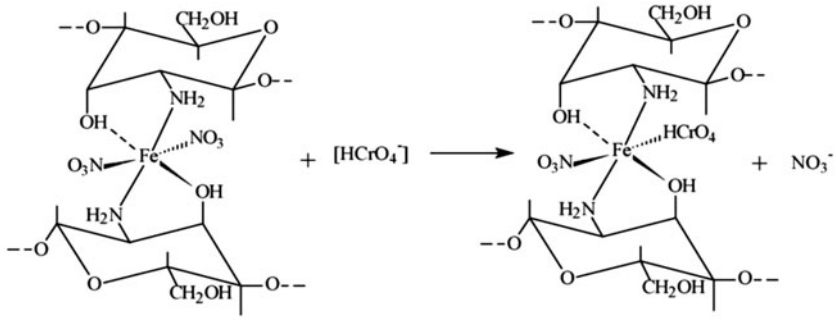

Scheme 1. Schematic diagram reaction between Fe–CCRB and Cr (VI) ions.

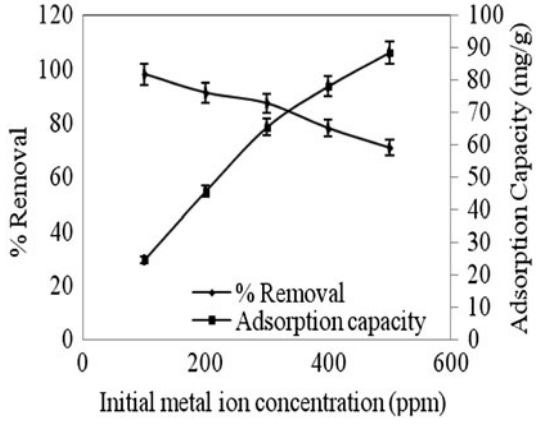

Fig. 6. Effect of initial metal ion concentration on adsorption capacity, and percentage removal of Cr (VI) ions by Fe–CCRB ($m = 0.1$ g, $v = 25$ ml, pH 2).

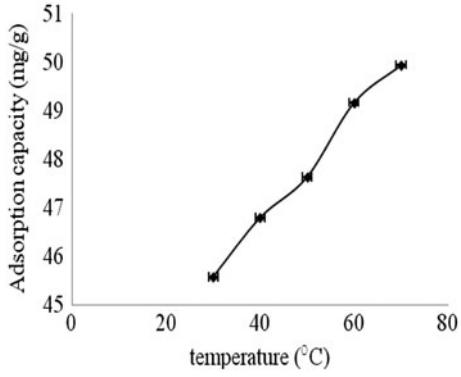

Fig. 7. Effect of temperature on adsorption capacity and percentage removal of Cr (VI) ions by Fe–CCRB ($m = 0.1$ g, $C_0 = 200$ mg/l $v = 25$ ml, pH 2).

applied to describe the equilibrium characteristics of adsorption of Cr (VI) ions by Fe–CCRB. In the Langmuir equation, θ (mg/g) is the measure of adsorbed quantity under the experimental conditions and b is a constant related to the energy of adsorption. In Freundlich isotherm, n is indicative of bond energies between metal ion and the adsorbent and K is related to bond strength. a and b are Temkin constants. B $(cm^3/mg)^g$ and g are Redlich-Peterson constants.

The nonlinear chi square analysis [37] was used to compare all the isotherms. The mathematical equation was given by Eq. (3):

$$x^2 = \sum \frac{(q_e - q_{e,m})^2}{q_e} \quad (3)$$

where $q_{e,m}$ is the equilibrium capacity obtained by calculation from model (mg/g) and q_e is the equilibrium capacity (mg/g) determined from the experimental data. If data from model are similar to the experimental data then x^2 would be a small number and vice versa [37]. In linear analysis, the different forms of equation would affect the regression coefficient (r) and coefficient of determination (r^2) value significantly, and this will affect the final determination. This can be avoided by using nonlinear chi square test analysis.

The linearized form of isotherms, values of constants, coefficient of determination (r^2), regression coefficient (r), and chi square test analysis (x^2) are given in Table 2.

Fig. 8 shows the comparison between theoretical isotherms and experimental data obtained for adsorption of Cr (VI) ions using Fe–CCRB. It is observed that the Freundlich and Redlich Peterson isotherms almost overlapped and seemed to be the best fitting models for the experimental data. Correspondingly, the chi square test analysis also showed that the x^2 values for Freundlich and Redlich Peterson isotherms are very low and almost identical when compared with Langmuir and Temkin isotherms. This reveals the multilayer adsorption of Cr (VI) ions on Fe–CCRB adsorbent.

3.8. Adsorption kinetics

In order to investigate the rate of adsorption process of chromium by Fe–CCRB, three different

Table 2
Summary of parameters for various isotherm models

Isotherms	Equation	Constants	r^2	r	x^2
Langmuir	$\frac{C_e}{q_e} = \frac{1}{b.\theta} + \frac{C_e}{\theta}$	θ (mg g^{-1}) = 94.4, b (L mg^{-1}) = 0.071	0.9897	0.9948	16.59
Freundlich	$\ln q_e = \ln K + \frac{1}{n}\ln C_e$	$1/n$ = 0.3027, K (mg g^{-1}) = 20.1	0.9914	0.9956	0.561
Temkin	$q_e = a + b\ln C_e$	b = 14.88, a (1/g) = 11.042	0.965	0.9823	2.026
Redlich-Peterson	$\ln\left(A\frac{C_e}{q_e} - 1\right) = g\ln(C_e) + \ln B$	g = 0.7297, B = 4.04,	0.9983	0.9991	0.517

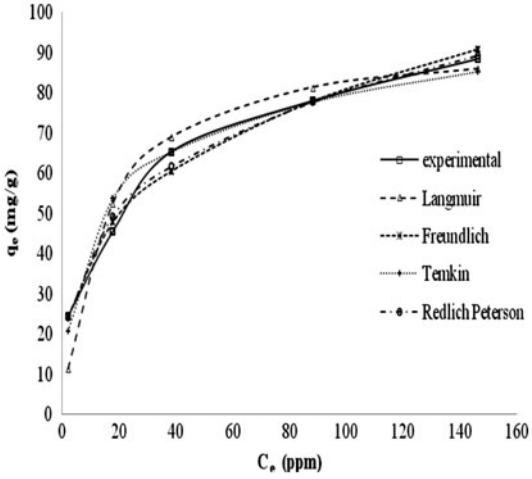

Fig. 8. Theoretical isotherms and experimental data for adsorption of Cr (VI) ions using Fe–CCRB.

kinetic models, such as pseudo-first-order kinetics, pseudo-second-order kinetics, and simple elovich kinetics were tested [38]. The linearized form of adsorption kinetics and their parameter values are given in Table 3.

In pseudo-first-order kinetics, q_t is the adsorbed quantity at time t (mg/g) and K_{1ad} is the pseudo-first-order rate constant in min^{-1}. In pseudo-second-order kinetics, K_{2ad} is the pseudo-second-order rate constant in 1/mol s. In simple elovich kinetics, α and β are the simple elovich kinetic constants.

Table 3
Summary of constants for various kinetic models

Kinetic model	Equation	Constant	Value
Pseudo-first-order	$\ln(q_e - q_t) = \ln q_e - K_{1ad}t$	K_{1ad}(min^{-1})	0.0695
		R^2	0.8131
Pseudo-second-order	$\frac{t}{q_t} = \frac{1}{K_{2ad}.q_e^2} + \frac{t}{q_e}$	K_{2ad} (g mg^{-1} min)	0.01
		q_e (mg/g) = 25	25
		R^2	0.999
Simple Elovich	$q_t = \alpha + \beta\ln t$	β	4.8153
		α	1.9623
		R^2	0.9432

From the table, it is confirmed that the adsorption of Cr (VI) ions using Fe–CCRB followed the pseudo-second-order reaction and is shown in Fig. 9. The pseudo-second-order model indicates that the adsorption of Cr (VI) ions on the surface of Fe–CCRB represented two phase reaction, such as rapid adsorption for shorter duration in initial stage followed by slow adsorption for longer duration.

Several investigators [39,40] reported that the fast reaction may be due to chemisorption involving valence forces through exchange or sharing of electron between the adsorbent and adsorbate. The slow reaction is due to the diffusion of ions into the adsorbent. Hence, the rate limiting step is finalized as chemisorption.

3.9. Intraparticle diffusion

The possibility of intraparticle diffusion [38] was explored by using the intraparticle diffusion model as given in Eq. (4).

$$q_t = K_{id}t^{1/2} + C \tag{4}$$

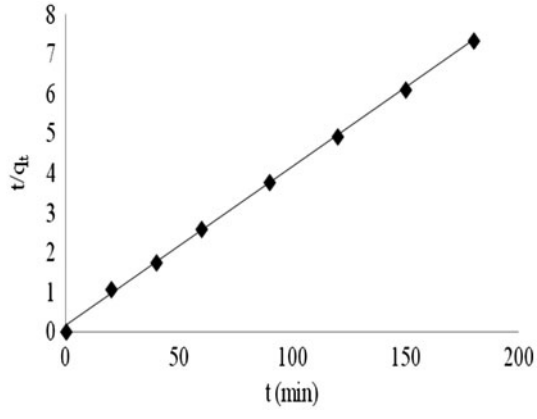

Fig. 9. Pseudo-second-order kinetics for adsorption of Cr (VI) ions using Fe–CCRB.

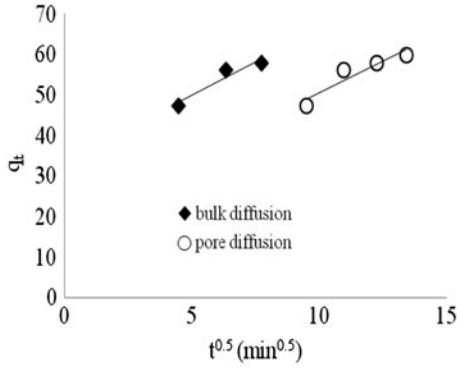

Fig. 10. Intraparticle diffusion for adsorption of Cr (VI) ions using Fe–CCRB.

where K_{id} is the intraparticle diffusion rate constant in $mg\,g^{-1}\,min^{-1/2}$ and C is the intercept. According to Eq. (4), a plot of q_t vs. $t^{1/2}$ provides a straight line with a slope K_{id} and intercept C when an adsorption mechanism follows the intraparticle diffusion process.

From Fig. 10, it is observed that there are two separate regions i.e. the initial portion is attributed to the bulk diffusion ($K_{id,1}$) and the final portion to intraparticle diffusion ($K_{id,2}$), which is also evident from the experimental data followed by Freundlich isotherm (multilayer adsorption).

The values of K_{id1}, K_{id2}, C_1, and C_2 using Eq. (4) were found to be $3.3136\,mg\,g^{-1}\,min^{-1}$, $3.0999\,mg\,g^{-1}\,min^{-1}$, 33.27, and 19.60, respectively, from Fig. 10.

3.10. Mass transfer studies

The mass transfer equation [41] is generally expressed by Eq. (5)

$$C_0 - C_t = De^{K_0 t} \tag{5}$$

where C_0 is the initial metal ion concentration ($mg\,dm^{-3}$), C_t is the metal ion concentration at time t, D is a fitting parameter, K_0 is the adsorption constant in min^{-1} which is related to the mass transfer adsorption coefficient K, $K_0 = Km$, where m is the mass of the adsorbent (g).

A linearized form of equation is given in Eq. (6)

$$\ln(C_0 - C_t) = \ln D + K_0 t \tag{6}$$

A plot of $\ln(C_0 - C_t)$ vs. time should give a linear relationship from where the constants $\ln D$ and K_0 can be determined from the slope and intercept of the plot, respectively.

Fig. 11 shows a plot of $\ln(C_0 - C_t)$ vs. time. The fitting parameter $\ln D$, the adsorption constant K_0, and

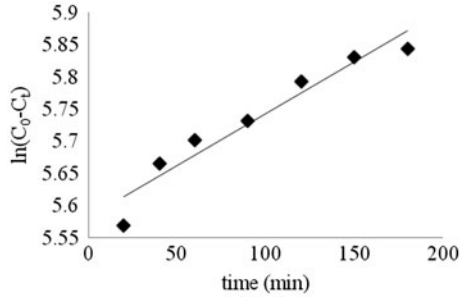

Fig. 11. Mass transfer kinetics for adsorption of Cr (VI) ions using Fe–CCRB.

the mass transfer adsorption coefficient value K computed from the slope and intercept are 5.5816, $0.0064\,min^{-1}$, and 0.00064 ($g\,L^{-1}\,min^{-1}$), respectively.

3.11. Thermodynamic parameters

The thermodynamic parameters [42] for the adsorption of Cr (VI) ions were determined using the following Eqs. (7)–(9):

$$K_D = \frac{q_e}{C_e} \tag{7}$$

$$\Delta G^\circ = -RT \ln K_D \tag{8}$$

$$\ln K_D = \Delta S^\circ / R - \Delta H^\circ / R \times T \tag{9}$$

where K_D is the distribution coefficient for the adsorption in g/l, ΔG° is the Gibbs free energy in J/mol, R is the gas constant in J/mol K, T is the absolute temperature in K, ΔS° is the entropy change in $J\,mol^{-1}\,K^{-1}$, and ΔH° is the enthalpy change in KJ/mol. A linear plot of $\ln K_D$ vs. $1/T$ was drawn. The value of ΔH° and ΔS° were obtained from the slope and intercept of the plot.

The thermodynamic constants were determined from Fig. 12 and the results for various temperatures

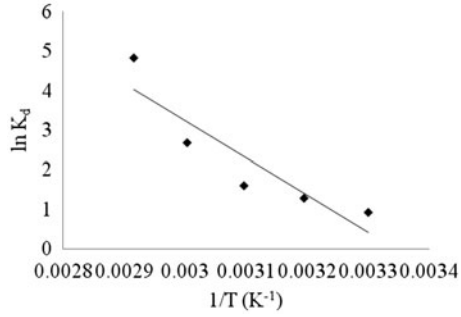

Fig. 12. Determination of Thermodynamic parameters ($C_0 = 200\,mg/l$, $m = 0.2\,g$, speed = 200 rpm, pH 2).

Table 4
Thermodynamic parameters for the adsorption of Cr (VI) ions using Fe–CCRB at different temperatures

S. no	T (K)	ΔG^o (J/mol)	ΔH^o (KJ/mol)	ΔS^o (J mol^{-1} K^{-1})
1	303	−2,382.95		
2	313	−3,370.93		
3	323	−4,342.69	78.22	261.6
4	333	−7,453.70		
5	343	−13,814.04		

are listed in Table 4. The positive values of ΔH° for all the temperatures indicate the feasibility of the process and the reaction is endothermic. The positive value of ΔS° indicate the occurrence of structural change on the surface of the adsorbent and increased randomness during the adsorption process. The negative values of Gibbs free energy ΔG^o change indicate the feasibility and spontaneous nature of adsorption.

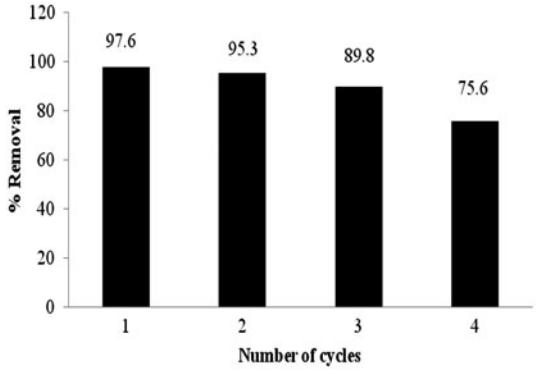

Fig. 13. Percentage removal on regeneration of Fe–CCRB.

4. Regeneration studies

Desorption studies were also conducted to explore the feasibility of recycling the adsorbents and recovery of the metal resources. NaOH was used for the stripping section. Desorption experiments were conducted by mixing 0.6 g of spent adsorbent with 25 ml of 1 M NaOH. In order to determine the reusability of the adsorbent, the adsorbent was taken out from the solution, washed with double distilled water, and protonated with 0.1 M HCl. Consecutive adsorption and desorption studies were repeated four times by using the same adsorbent and shown in Fig. 13. It was found that there was only little change in percentage removal that shows the stability of the adsorbent.

5. Comparison with other adsorbents

The experiments were also conducted with other adsorbents for the adsorption of Cr (VI) ions, such as acid-treated carbonized rice husk, ozone-treated carbonized rice husk, chitosan-coated carbonized rice husk, glutaraldehyde cross-linked chitosan carbonized rice husk composite, epichlorohydrin cross-linked chitosan carbonized rice husk composite and ethylamine-modified chitosan carbonized rice husk composite beads.

The maximum percentage removal and adsorption capacity of Cr (VI) ions were found to be more for

Table 5
Comparison with other adsorbents

Adsorbents	Percentage removal	q_e (mg/g)
Carbonized rice husk	20.2 (25 ml of 100 ppm, 0.1 g dosage, pH 2)	4.9
Acid treated carbonized rice husk	47.3 (25 ml of 100 ppm, 0.1 g dosage, pH 2)	11.8
Ozone treated carbonized rice husk	65.9 (25 ml of 100 ppm, 0.1 g dosage, pH 2)	16.5
Glutaraldehyde cross-linked chitosan carbonized rice husk composite	87.9 (25 ml of 100 ppm, 0.1 g dosage, pH 2)	22.0
Epichlorohydrin cross-linked chitosan carbonized rice husk composite	81.4(25 ml of 100 ppm, 0.1 g dosage, pH 2)	20.4
Ethylamine-modified chitosan carbonized rice husk composite beads	96.0 (25 ml of 100 ppm, 0.1 g dosage, pH 2)	24.0
Fe–CCRB	98.3(25 ml of 100 ppm, 0.1 g dosage, pH 2)	24.5
	87 (300 ppm)	65
	70 (500 ppm)	86

Fe–CCRB when compared with other adsorbents and the results are reported in Table 5.

6. Conclusion

Fe–CCRB is an effective adsorbent for the removal of chromium from aqueous solutions. There is no significant change in the BET surface area. A SEM image reveals that the Fe–CCRB particles have narrow size distribution, spherical-shaped with very small cavities and rough surfaces. FTIR was done before and after adsorption. The shifting in peaks revealed that the Cr (VI) ions were attached to the various functional groups present in Fe–CCRB. Adsorption of Cr (VI) ions was highly pH dependent and the results showed that the optimum pH for the removal of Cr (VI) ions was obtained at pH 2. The maximum percentage removal of 98% at 100 ppm and adsorption capacity of 88 mg/g at 500 ppm were obtained. Equilibrium adsorption data for chromium removal was best represented by Freundlich isotherm and the same is confirmed in intraparticle and mass transfer diffusion studies. Adsorption kinetics was found to fit suitably in a pseudo-second-order kinetic model. A thermodynamic study reveals the endothermic, randomness, and spontaneous nature of the adsorption processes.

Acknowledgment

The author gratefully acknowledges and thanks those who have been instrumental in the successful completion of this project.

References

[1] J.R. Utrilla, I.B. Toledo, M.A.F. Gercia, C.M. Castilla, Bioadsorption of Pb(II), Cd(II) and Cr(VI) on activated carbon from aqueous solutions, Carbon 41 (2003) 323–330.
[2] U.K. Garg, M.P. Kaur, D. Sud, D.V K. Garg, Removal of hexavalent chromium from aqueous solution by adsorption on treated sugarcane bagasse using response surface methodological approach, Desalination 249 (2009) 475–479.
[3] EPA Environmental Pollution Control Alternatives EPA/625/5-90/25, EPA/625/4-89/023, Environmental Protection Agency Cincinaati OH USA, 1990.
[4] M. Owald, M.K. Aroua, W.A. Daud, S. Baroutian, Removal of hexavalent chromium-contaminated water and wastewater: A review, Water Air Soil Pollut. 200 (2009) 59–77.
[5] L. Monser, N. Adhoum, Modified activated carbon for the removal of copper, zinc, chromium and cyanide from wastewater, Sep. Purif. Technol. 26 (2002) 137–146.
[6] K.Y. Foo, B.H. Hameed, Preparation and characterization of AC from melon (Citrullus Vulgaris) seed hull by microwave induced NaOH activation, doi: 10.1080/1944 3994.2012. 696826.
[7] S. Chatterjee, D. Lee, S. Lee, S.H. Woo, Congo red adsorption from aqueous solutions by using chitosan hydrogel beads impregnated with nonionic or anionic surfactant, Bioresour. Technol. 100 (2009) 3862–3868.
[8] E. Thirunavukkarasu, K. Palanivelu, Biosorption of Cr(VI) from plating effluent using marine algal mass, Ind. J. Biotechnol. 16 (2007) 359–364.
[9] M. Yigitoglu, M. Arslan, Adsorption of hexavalent chromium from aqueous solutions using 4-vinyl pyridine grafted poly (ethylene terephthalate) fibers, Polym. Bull. 55 (2005) 259–268.
[10] E.I. El-Shafey, Behaviour of reduction–sorption of chromium (VI) from an aqueous solution on a modified sorbent from rice husk, Water Air Soil Pollut. 163 (2005) 81–102.
[11] H. Jaman, D. Chakraborty, P. Saha, A study of the thermodynamics and kinetics of copper using chemically modified rice husk, Clean 37 (2009) 704–711.
[12] N. Yalc, V. Sevinc, Studies of the surface area and porosity of activated carbons prepared from rice husks, Carbon 38 (2000) 1943–1945.
[13] Y. Guo, S. Yang, K. Yu, J. Zhao, Z. Wang, H. Xu, The preparation and mechanism studies of rice husk based porous carbon, Mater. Chem. Phys. 74 (2002) 320–323.
[14] Y. Guo, K. Yu, Z. Wang, H. Xu, Effects of activation conditions on preparation of porous carbon from rice husk, Carbon 41 (2000) 1645–1687.
[15] A.K. Rout, A. Satapathy, Study on mechanical and tribo-performance of rice-husk filled glass–epoxy hybrid composites, Mater. Des. 41 (2012) 131–141.
[16] S.M. Nomanbhay, K. Palanisamy, Removal of heavy metal from industrial wastewater using chitosan coated oil palm shell charcoal, E.J. Biotechnol. 8 (2005) 43–53.
[17] S. Maghsoodlooa, B. Noroozia, A.K. Haghia, G.A. Sorial, Consequence of chitosan treating on the adsorption of humic acid by granular activated carbon, J. Hazard. Mater. 191 (2011) 380–387.
[18] M. Hasan, A.L. Ahmad, B.H. Hameed, Adsorption of reactive dye onto cross-linked chitosan/oil palm ash composite beads, Chem. Eng. J. 136 (2008) 164–172.
[19] J.K. Warcholc, E.T. Repoa, A. Kurniawana, M.E.T. Sillanpaa, Adsorption of Co(II) and Ni(II) by EDTA- and/or DTPA-modified chitosan: Kinetic and equilibrium modelin, Chem. Eng. J. 161 (2010) 73–82.
[20] C. Septhum, S. Rattanaphani, J.B. Bremner, V. Rattanaphani, An adsorption study of Al (III) ions onto chitosan, J. Hazard. Mater. 148 (2007) 185–191.
[21] G. Crini, P.M. Badot, Application of chitosan, a natural aminopolysaccharide, for dye removal from aqueous solutions by adsorption processes using batch studies: A review of recent literature, Prog. Polym. Sci. 33 (2008) 399–447.
[22] A.C. Zimmermann, A. Mecabo, T. Fagundes, C.A. Rodrigues, Adsorption of Cr (VI) using Fe–crosslinked chitosan complex (Ch–Fe), J. Hazard. Mater. 179 (2010) 192–196.
[23] H. Guolin, Y. Chuo, Z. Kai, S. Jeffrey, Adsorptive removal of copper ions from aqueous solution using cross-linked magnetic chitosan beads, Chin. J. Chem. Eng. 17 (2009) 960–966.
[24] K.P. Singha, S. Guptaa, A.K. Singh, S. Sinha, Optimizing adsorption of crystal violet dye from water by magnetic nanocomposite using response surface modeling approach, J. Hazard. Mater. 186 (2011) 1462–1473.
[25] W.S.W. Ngah, M.A.K.M. Hanafiah, S.S. Yong, Adsorption of humic acid from aqueous solutions on cross linked chitosan–epichlorohydrin beads: Kinetics and isotherm studies, Colloids Surf. B. 65 (2008) 18–24.
[26] L. Zhoua, Y. Wang, Z. Liua, Q. Huang, Characteristics of equilibrium, kinetics studies for adsorption of Hg(II), Cu(II), and Ni(II) ions by thiourea-modified magnetic chitosan microspheres, J. Hazard. Mater. 161 (2009) 995–1002.
[27] Y. Tao, L. Ye, J. Pan, Y. Wang, B. Tang, Removal of Pb(II) from aqueous solution on chitosan/TiO_2 hybrid film, J. Hazard. Mater. 161 (2009) 718–722.
[28] M. Sindhu, K.M. Meera, S. Begum, S. Sugashini, A comparative study of surface modification in carbonized rice husk by acid treatment, Desalin. Water Treat. 45 (2012) 170–176.
[29] J.M. Lee, K. Palanivelu, Y.S. Lee, Removal of hexavalent chromium on deposited activated carbon, Solid State Phenom. 135 (2008) 85–88.

[30] M. Christine, U.F. Sala, U.P. Sala, Quantitative determination of hexavalent chromium in aqueous solutions by UV–vis spectrophotometer, Central Eur. J. Chem. 5 (2007) 1083–1093.
[31] M.S. Siboni, M.R. Samarghandi, S. Azizian, W.G. Kim, S.M. Lee, The removal of hexavalent chromium from aqueous solutions using modified holly sawdust: Equilibrium and kinetics studies, Environ. Eng. Res. 16 (June) (2011) 55–60.
[32] M.Y. Chang, R.S. Juang, Adsorption of tannic acid, humic acid, and dyes from water using the composite of chitosan and activated clay, J. Colloid Interf. Sci. 278 (2004) 18–25.
[33] S. Mor, K. Ravindra, N.R. Bishnoi, Adsorption of chromium from aqueous solution by activated alumina and activated charcoal, Biores. Technol. 98 (2007) 954–957.
[34] R. H. Krishna, A.V.V.S. Swamy, Investigation on the adsorption of hexavalent chromium from the aqueous solutions using powder of papaya seeds as a sorbent, Int. J. Environ. Sci. Res. 2 (2012) 119–125.
[35] Z. Aksu, E. Kabasakal, Batch adsorption of 2,4-dichlorophenoxy-acetic acid (2,4-D) from aqueous solution by granular activated carbon, Sep. Purif. Technol. 35 (2004) 223–240.
[36] Z.E.S. EI-Ashtoukhy, N.K. Amin, O. Abdelwahab, Removal of lead (II) and copper (II) from aqueous solution using pomegranate peel as a new adsorbent, Desalination 223 (2008) 162–173.
[37] Y.S. Ho, Selection of optimum sorption isotherm, Carbon 42 (2004) 2115–2116.
[38] A.A. Attia, S.A. Khedr, S.A. Elkholy, Adsorption of chromium ion (VI) by acid activated carbon, Braz. J. Chem. Eng. 27 (2010) 183–193.
[39] P. Saueprasearsit, Adsorption of chromium (Cr+6) using durian peel, International conference on biotechnology and environment management, IPCBEE 18 (2011).
[40] L. Hai-Jun, L. Mao-Tian, Z. Jin-Li, A kinetic study on the adsorption of Cr (VI) onto a natural material used as land fill liner, Elect. J. Geotech. Eng. 14 (2009) 1–10.
[41] A.A. Augustin, B.D. Orike, A.D. Edidiong, Adsorption kinetics and modeling of Cu (II) ion sorption from aqueous solution by mercaptoacetic acid modified cassava (manihot sculenta cranz) wastes, EJEAFChe 6 (2007) 2221–2234.
[42] Z. Sadaoui, S. Hemidouche, O. Allalou, Removal of hexavalent chromium from aqueous solutions by micellar compounds, Desalination 249 (2009) 768–773.